Thermal expansion, pressure and non-isostatic effects on crustal thickness determination using a gravimetric-isostatic model:

A case study in South America

Mohammad Bagherbandi[1,2], Yongliang Bai[3], Majid Abrehdary[1], Lars E. Sjöberg[1], Robert Tenzer[5], Silvia Miranda[4], Juan M. A. Sanchez[4]

[1] Division of Geodesy and Satellite Positioning, Royal Institute of Technology (KTH), SE-100 44 Stockholm, Sweden.

[2] Department of Industrial Development, IT and Land Management, University of Gävle, SE-801 76 Gävle, Sweden.

[3] Key Laboratory of Marine Geology and Environment, Institute of Oceanology, Chinese Academy of Sciences No.7 Nanhai Rd, Qingdao 266071, China.

[4] Departamento de Geofísica y Astronomía, FCEFN. Universidad Nacional de San Juan, Meglioli 1160 Sur, 5400. Rivadavia, San Juan, Argentina.

[5] School of Geodesy and Geomatics, Wuhan University, 129 Luoyu Road, Wuhan, China.

Corresponding author. Mohammad Bagherbandi. Address: Division of Geodesy and Satellite Positioning, Royal Institute of Technology (KTH), Drottning Kristinas väg 30, 10044 Stockholm, Sweden. E-mail address: mohbag@kth.se.

Abstract

In this study, we show a new gravimetric-isostatic crustal thickness model via the recent combined satellite only GOCO03S and ETOPO1 topographic models using the Vening Meinesz-Moritz hypothesis in South America and the surrounding ocean basins. Accordingly, in order to solve the gravimetric problem of isostasy for finding the Moho parameters, we present a new method which primarily filters the disturbing gravity disturbance signals from the topography and density heterogeneities related to bathymetry, ice, sediments and masses below crust. As less appreciated are the effects of the lithospheric thermal state on continental or oceanic areas. Hence we develop this method by which thermal contribution from the gravity data may be removed. We find that thermal effect, which varies 0 to -274 with standard deviation 71 mGal, has a significant contribution on gravimetric crustal thickness determination. Ignoring the thermal effect and other disturbing signals from deeper mantle masses provide large bias in determination of the crust boundary. The bias will be reached up to 4 km in rms.

Key words: Crust, Gravity inversion, Moho, Non-isostatic effects, Thermal compensation, Upper mantle.

1. Introduction

The Earth's crustal thickness can be determined using seismic and gravimetric methods (cf. Bagherbandi 2011). Gravity data are recently more applicable for the crustal thickness determination because of their global coverage. Assuming that the Earth's topographic masses are isostatically compensated by the masses in lower layers, combination of isostatic hypotheses with gravity data can be one of the methods to model the Earth's crust (Sjöberg 2009). Among isostatic models Vening Meinesz' (1931) model is closer to the real form of crust because Vening Meinesz' approach considers a regional isostatic compensation. The main problems with the gravimetric-isostatic models are some disturbing gravity signals (cf. Bagherbandi and Sjöberg 2013) from lower layers of the Earth and assuming uniform density (for topography, sediments, ice and water). Therefore, the gravity data should be corrected by additional corrections. In this study we use the corrections to filter the disturbing signals in the gravity disturbances in the Vening Meinesz-Moritz (VMM) inverse problem (cf. Sjöberg 2009) of isostasy for finding the Moho depths (cf. Bagherbandi et al. 2013 and Tenzer et al. 2014) following the latest development in isostatic theory, we address here some major aspects related to isostatic gravity disturbances. The computation of these types of gravity data to model the crustal thickness requires the application of the stripping gravity correction (Tenzer et al. 2009, 2012) due to sediments which represent a significant amount of gravitational signal over the oceans. The sediment density structures under continents are very important to consider for improving the gravimetric-isostatic model. The other significant gravity signals are the signals due to the density structure of ice and topography and thermal effect (cf. Bai et al. 2014 and Wang et al. 2011). These density variations are implicitly in the gravity data. We evaluate the methodology by application to the South America where there are many basins and their sedimentary fill is large. Here we go one step further to filter the thermal and pressure effects from the gravity data to model the crust. Affected by thermal expansion and pressure compression effect, the lithospheric mantle density is not constant but changing according to the temperature and pressure fields (Chapman and Pollack, 1977; Kimbell et al., 2004), and some applications demonstrate that the Moho topography inversion accuracy could be improved by considering thermal and or pressure effects on gravity field (Afonso et al., 2008; Chappell and Kusznir, 2008). In this paper will add similar corrections for mapping Moho topography by gravity inversion.

2. Gravity inversion using the VMM

One of the fundamental challenges of geophysical study is to determine the geometry of subsurface structure (density interfaces) using gravity disturbance data. One such important application is to depict crust–mantle boundary (Moho) from surface gravity disturbance. The solution of this problem can be categorized into two main modelling techniques: forward and inverse (Ebbing et al., 2001), which the latter is only regarded in this study.

2.1 Vening Meinesz-Moritz' method

Based on Sjöberg (2009) we now start the basic isostatic condition for gravity disturbance,

$$\delta g_I(P) = \delta g_B^R(P) + A_C(P) = 0, \tag{1}$$

Here $\delta g_B^R(P)$ is the Bouguer gravity disturbance corrected for the gravitational contributions of topography/bathymetry and density contrasts of the oceans, ice and sediments and A_C is the gravitational attraction of isostatic compensation masses (Moritz 1990 Chapter 8, Sjöberg 2009). The VMM problem, based on formula above, can be formulated by the non-linear integral equation

$$R\iint_\sigma K(\psi, s)\, d\sigma = -\left[\delta g_B^R(P) + A_{C0}(P)\right] / G\Delta\rho, \tag{2}$$

where $K(\psi, s)$ is kernel function of the integral, R is the mean Earth radius, σ is the unit sphere, ψ is the geocentric angle, s is the a simple function of the Moho depth D, which is the unknown of the integral equation, G is Newton's gravitational constant, $\Delta\rho$ is the Moho density contrast, and $A_{C0}(P)$ is the nominal compensation attraction with D_0 as the nominal Moho depth.

2.2 Corrections to gravity disturbances

At this stage, our objective is to compute the gravity disturbances corrected due to the gravitational contributions of topography, and density variation of ocean (bathymetry), ice and the crustal residual density. Accordingly, Tenzer et al. (2012a) and Tenzer et al., (2014) developed and applied the uniform mathematical formalism for computing the gravity corrections of density variation within the Earth's crust, such as topographic, bathymetric, ice, sediment with a spherical resolution complete to degree n of spherical harmonics and up to the third-order terms of a binomial. In order to simplify the computation, the spherical harmonic

analysis and synthesis for determination of the effects of major known crustal density structures are given below:

$$L_{\mathrm{nm}} = \frac{1}{4\pi}\iint_{\sigma}\left(density\right)^{q}\left(thickness\right)^{q} Y_{nm}\left(Q\right) d\sigma, \tag{7}$$

Here q denotes the topography, bathymetry, ice and sediment

$$\delta g^{q} = \frac{GM}{R^{2}}\sum_{n}^{n_{max}}\left(n+1\right)\sum_{m=0}^{n} L_{nm} Y_{nm}\left(P\right) \tag{8}$$

The computation of the gravity disturbances is performed here in spectral domain using methods for a spherical harmonic analysis and synthesis of gravity field (cf. Tenzer et al. 2009a and 2009b; Bagherbandi et al. 2013).

$$\delta g_{B}^{R} = \delta g + \delta g^{t} + \delta g^{b} + \delta g^{i} + \delta g^{s} \tag{9}$$

where δg^{t}, δg^{b}, δg^{i}, and δg^{s} are the gravity disturbance corrections due to the gravitational contributions of topography and density variations of ocean (bathymetry), ice and sediments (cf. Bagherbandi et al. 2013).

2.3 Thermal effect due to lithosphere mantle density

Several methods have been proposed for oceanic lithospheric mantle temperature calculation and consequently lithosphere thermal gravity anomaly, for example, by McKenzie (1978), Parsons and Richter (1980), Bouhifd et al. (1996), McKenzie et al. (2005), Afonso et al. (2008) and Bai et al. (2014). Thermal isostasy is the geodynamic process whereby regional variations in the lithospheric thermal regime cause changes in elevation. Elevation changes result from variations in rock density in response to thermal expansion. Therefore the lithospheric mantle density is not constant, the density variation should be taken into account for gravity study.

The density of lithospheric mantle in the thermal regime would be reduced by the effect of thermal expansion, on the other hand, the density also could be increased affected the pressure-driven compression due to the loading martials. When the buried depth of target lithospheric mantle unit for density modeling is z, the density of lithospheric mantle could be evaluated by

$$\rho_{z} = \rho_{0}[-\alpha\left(T_{z}-T_{0}\right)+\beta_{T_{z}}\left(P_{z}-P_{0}\right)] \tag{10}$$

where, ρ_{0} (=3.3 g/cm^{3}) is the lithospheric mantle density with normal temperature T_{0} (=273 K) and normal pressure P_{0} (101 KPa, the standard atmospheric pressure), α is the thermal

expansion coefficients and we set its value is $3.28\times10^{-5}K^{-1}$ constantly according to former studies (Bai et al., 2014; Chappell and Kusznir, 2008), β_{T_z} is the pressure-driven compressibility coefficient whose value is relevant to temperature, T_z and P_z is the temperature and pressure at depth z, respectively.

−Temperature field

According to the pure shear model (McKenzie, 1978), the temperature at depth z could be derived by

$$T_z = T_1\left(1-\frac{(a-\mathrm{z})}{a}+\frac{2}{\pi}\sum_{n=1}^{\infty}\frac{(-1)^{n+1}}{n}\left[\frac{\gamma}{n\pi}\sin\frac{n\pi}{\gamma}\right]\exp\left[\frac{-n^2t}{\tau}\right]\sin\frac{n\pi(a-\mathrm{z})}{a}\right) \tag{11}$$

where T_1 (= 1060 K) is the boundary temperature of lithosphere and asthenosphere, a (= 125 km) is equilibrium lithosphere (plate) thickness, τ (=62.8 Myr) is the lithosphere cooling thermal decay constant, t is crustal age, γ is lithosphere stretching factor (McKenzie, 1978; McKenzie et al., 2005). The oceanic crustal age could be estimated based on magnetic lineation and the continental crustal age is set constantly as 300 *Ma* in this study. The lithospheric stretching factor could be approximated by crustal stretching factor and $\gamma=\infty$ for the oceanic lithosphere (Chappell and Kusznir, 2008). The initial values of continental crustal stretching factors which are necessary for thermal modelling are based on crustal thickness mapped by gravity inversion without considering thermal expansion and pressure compression effects; and thus the thermal expansion effect can be calculated iteratively.

− Pressure-driven compressibility coefficient

The bulk modulus (K) could be simulated by a function of temperature, T, and it given by (Kroll et al., 2012):

$$K_T = 127.97-0.0232\times(T-300), \tag{12a}$$

Assuming this relation the pressure-driven compressibility coefficient (β_{T_z}) could be derived based on temperature value according to the inverse relationship between pressure-driven compressibility coefficient β_{T_z} and the bulk modulus (K_T)

$$\beta_{T_z} = 1/K_T. \tag{12b}$$

− Pressure field

Pressure value at depth z could be calculated based on the definition of lithospheric pressure P_z:

$$P_z = \int_0^z \rho(\mathrm{z}')\,\mathrm{dz}' \tag{13}$$

In space domain, the gravity disturbance due to thermal and pressure effects could be calculated by

$$\delta g^{TE}(P) = G\iint_{\sigma}\int_{R-z}^{R} \frac{(\rho_z - \rho_0)r}{l_P^3} dr d\sigma \tag{14}$$

Therefore, the gravity disturbance δg^{TE}, at point P on the earth surface, of lithospheric mantle density variations by thermal expansion effect and pressure-driven compression effect can be calculated by Eq. (14).

2.4 The non-isostatic effects

It is almost impossible to distinguish the crustal and mantle gravity field and geothermal modelling without additional data on the crustal structure (e.g., Kaban et al., 2004; Artiemeva, 2006; Artiemeva et al., 2006, Tesauro et al. 2008). In reality, Moho is not only formed by isostasy, but there are other causes, which affect the crustal thickness estimation. Using the isostatic hypothesis for determining the depth of crust causes some disturbing signals, non-isostatic effects (NIEs), which influence the crustal thickness determination. It is the effect of the masses beneath of the crust. Hence the NIEs are the gravitational effects that are caused by the deviation of Moho geometry from its isostatic model. Major parts of the long-wavelengths of the geopotential are caused by density variations in the Earth's mantle and core/mantle topography variations (Martinec, 1994). According to Bagherbandi and Sjöberg (2013) the isostatic assumption for compensating the topographic potential is inadequate, and other effects should be considered. Therefore the considered assumption Moritz (1990) and Sjöberg (2009) for Vening Meinesz' inverse problem in isostasy should be corrected by these effects. Bagherbandi and Sjöberg (2013) presented a solution to overcome to this problem. The correction of δg^{NIE} is given by subtracting the compensation potential obtained from seismic based Moho (e.g. CRUST1.0) and that obtained from gravity inversion (i.e. VMM), an estimate of the NIEs harmonic coefficients are obtained by:

$$c_{nm}^{NIE} = c_{nm}^{\mathrm{CRUST1.0}} - c_{nm}^{VMM}, \tag{15a}$$

where spherical harmonic coefficients c_{nm}^{j} (j=VMM , CRUST1.0) are given by:

$$\mathrm{c}_{nm}^{j} \approx \frac{3}{(2n+1)R\rho_e}\left[\left(\Delta\rho\left(D_j - D_0\right)\right)_{nm} + \frac{(n+2)\left(\Delta\rho(D_0^2 - D_j^2)\right)_{nm}}{2R}\right], \tag{15b}$$

and $\rho_e \approx 5.5$ g/cm^3 is the mean density of the Earth's mass. The spherical harmonic coefficients of $\Delta\rho\left(D_j - D_0\right)$, $\Delta\rho(D_0^2 - D_j^2)$ and $\Delta\rho(D_j^3 - D_0^3)$ are shown by $\left(\Delta\rho\left(D_j - D_0\right)\right)_{nm}$, $\left(\Delta\rho(D_0^2 - D_j^2)\right)_{nm}$ and $\left(\Delta\rho(D_j^3 - D_0^3)\right)_{nm}$. Now using the harmonic coefficients of c_{nm}^{NIE} , the NIEs on gravity can be found by:

$$\delta g^{NIE} = \frac{GM}{R^2}\sum_{n=0}^{n_{max}}(n+1)\left(\frac{R}{r_p}\right)^{n+2}\sum_{m=-n}^{n} c_{nm}^{NIE} Y_{nm}(P) \tag{16}$$

This implies that δg^{NIE} should be corrected on the isostatic gravity disturbance (δg_I), yielding the pure isostatic gravity disturbance. Finally, using the gravity corrections of density contrast within the Earth's crust (δg^t , δg^b , δg^i and δg^s), the non-isostatic (δg^{NIE}) and thermal effects (δg^{TE}) and, the isostatic gravity disturbance is given by:

$$\delta g_I(P) = \delta g_B^R(P) + A_C(P) + \delta g^{NIE}(P) + \delta g^{TE}(P) = 0 \tag{17}$$

3 Numerical study

3.1 Description of the data

The refined Bouguer gravity disturbances were generated for South American region from the recent combined satellite only model GOCO03S (Mayer-Gürr, et al. 2012), and the spherical harmonics of the normal gravitational field according to the parameters of the reference system GRS-80 (Moritz, 1980), complete to degree and order 180 of spherical harmonics. It deserves to be mentioned that by removing the gravitational contributions of topography and density variations of the oceans, ice sheets, sediment basins and also NIEs and thermal effects, the resulting Bouguer disturbance describes better the subsurface density effects including the

Moho boundary. In this context, firstly the generated gravity disturbances were corrected for the gravitational contributions of topography and density variations of the oceans, ice sheets and sediment basins which these corrections were provided by the ESCM180 Earth's spectral crustal model (see Tenzer et al., 2014) and thermal effects (Bai et al., 2014) and later on they were corrected for NIEs (see Bagherbandi and Sjöberg 2013).

The thermal correction was calculated using the oceanic crustal age grid (Müller et al., 2008; Seton et al., 2012), solid earth topographical heights from ETOPO1 data, total sediment thickness of the world's oceans and marginal seas by Divins (2003) and the global sediment thickness grid onshore by Dziewonski and Anderson (1981); the bathymetry and sediment thickness grids are used for Moho surface estimation.

To validate our estimated Moho depths, point-wise seismic data (obtained from Assumpcao et al. 2013) and seismic Moho model (CRUST1.0) in this region were used, respectively. Figure 1 shows the distribution of the point-wise seismic data and the solid Earth topography.

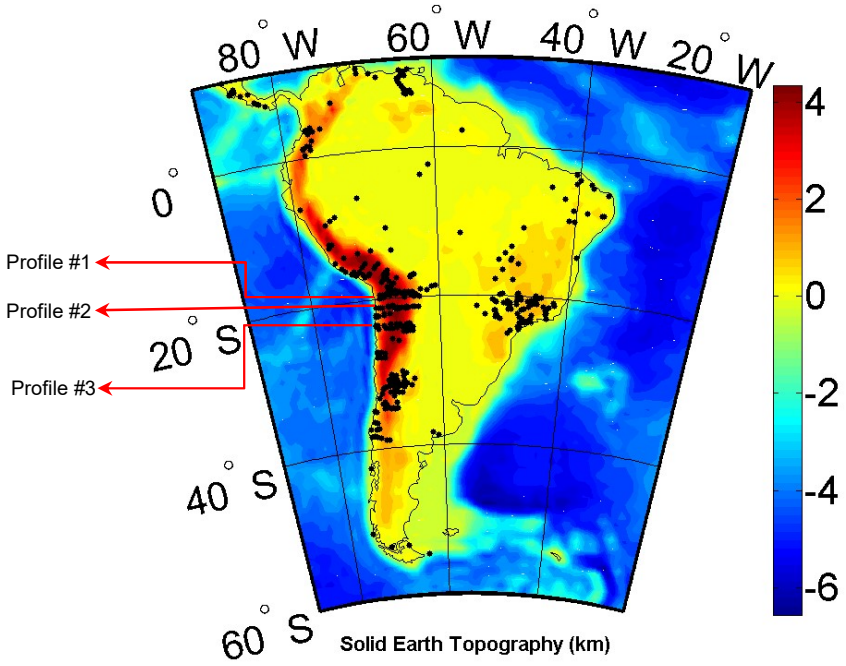

Figure 1. Point-wise seismic data presented by Assumpcao et al. (2013) and solid Earth topographical heights of South America generated from ETOPO1 data to degree and order of 180 corresponding to 1×1 arc-degree. Unit: km

3.2 Moho estimation of the South American region

In order to estimate the Moho depth, the selected region is bounded by latitude and longitude $-60^{\circ} \le \varphi \le 12^{\circ}$ and $-90^{\circ} \le \lambda \le -20^{\circ}$ respectively. Accordingly, we used the VMM method together with CRUST1.0 data to model the Moho depth, for the South American region. The reasons of using this area are: (a) this region contains reasonably accurate seismic Moho depths that can be used to validate our method and (b) also this region comprises both continental and marine regions and containing rough topography. From this numerical study, we illustrate that our inversion procedure would be suitable for local Moho depth estimations. The statistics of the numerical studies are given in Tables 1 and 2.

Table 1. Statistics of the effect of sediment, thermal compensation and NIE on the Moho depth and the gravity disturbances in South America. STD is the standard deviation of the estimated quantities.

Units	Quantities	Max.	Mean	Min.	STD
Km	D^{sediment}	-0.3	-2.0	-8.0	1.3
mGal	$\delta g^{\text{sediment}}$	168.1	42.9	6.3	27.6
Km	D^{TE}	13.1	3.7	0.0	3.4
mGal	δg^{TE}	0.0	-78.7	-274.3	71.8
Km	D^{NIE}	23.2	3.3	-13.8	5.1
mGal	δg^{NIE}	290.2	-68.5	-487.9	107.6

As can be seen from table above, $\delta g^{\text{sediment}}$, δg^{TE} and δg^{NIE} are the sediment effect, thermal effects and NIEs on gravity and D^{sediment}, D^{TE} and D^{NIE} are the sediment effect, thermal effects and NIEs on Moho depth, respectively.

Table 2. Statistics of the Moho depths estimated from Gravimetric-isostatic and seismic CRUST1.0 models in South America. STD is the standard deviation of the estimated quantities. RMS is the Root Mean Square.

Unit	Quantities	Max.	Mean	Min.	STD	RMS
k	D^{VMM}	76.33	23.44	10.46	13.9	

	$D^{CRUST1.0}$	69.51	21.75	9	12.98	
	$D_{NIE+TE}^{VMM-CRUST1.0}$	14.90	-0.5	-15.7	2.7	2.8
	$D_{NIE\ only}^{VMM-CRUST1.0}$	16.2	3.2	-14.5	3.4	4.7
	$D_{NIE+TE}^{VMM-PWSD}$	11.9	-0.8	-12.2	4	4.2
	$D_{NIE\ only}^{VMM-PWSD}$	11.6	-1.5	-12.9	4.2	4.5

As seen in the table, the VMM Moho depth varies between 10 and 76 km with a global average and standard deviation of 23 km and 14 km and corresponding Moho depths of the CRUST1.0 for this area varies between 9 and 69 km with a global average and standard deviation of 22 km and 13 km, respectively. In order to assess our results, first the estimated gravimetric-isostatic Moho depths (before and after applying the thermal effect) were compared with CRUST1.0 model and then with seismic-refraction data. The RMS of these differences between the VMM and CRUST1.0 Moho depths and the point-wise seismic data (PWSD) are of the order of 4.7 and 4.5 km and of 2.8 and 4.2 km before and after applying the thermal effect, respectively. A possible explanation for such improvement could be attributed to the applying the thermal effect which truncates the long-wavelength character more.

4 Analysis of the results

4.1 General analysis

As emphasized, the gravity inversion can be used to obtain local Moho depths that have better resolution and accuracy than global Moho depths. Accordingly, we apply the VMM method discussed in the previous section for determining Moho depths in the South American region. The detailed analyses of the results are plotted in this section.

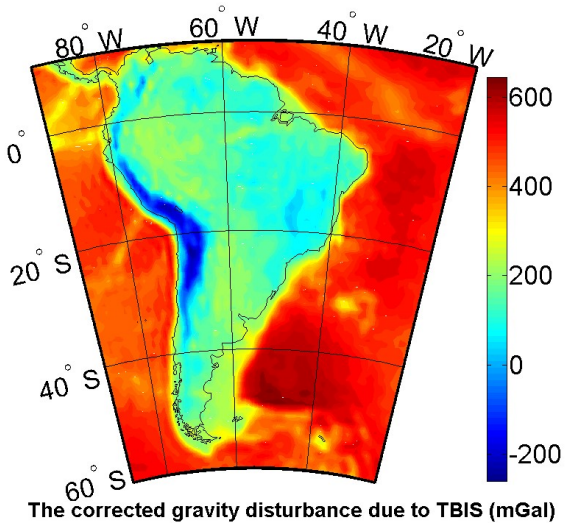

Figure 2. The corrected gravity disturbance (due to the gravitational contributions of topography and density variation of ocean, ice and sediments) with resolution 1×1 arc-degree. Unit: mGal

Figure 2 maps Bouguer gravity disturbances corrected due to the gravitational contributions of topography and density variation of ocean, ice and sediments. As mentioned, the refined gravity disturbances used as the input gravity data for finding the Moho depths should comprise only the gravitational signal of the Moho geometry. In this context, at the first step, we removed the topographic, bathymetry, ice and sediment gravity effects from the Bouguer disturbances compiled from GOCO03S and ETOPO1 global models. Also in Fig. 2 one can observe that the refined spherical Bouguer gravity disturbances are negative along the continental margin with extreme values of less than -200 mGal in high mountains, while oceanic areas are mostly changed to positive gravity values. The figure implies that the topographic masses are generally isostatically compensated by mass anomalies in the lithosphere (Watts 2001).

4.2 Moho depths vs sediment, thermal and non-isostatic effects

As we explained already, we firstly remove the topographic, bathymetry, ice and sediment gravity effects from the Bouguer disturbances but it should be noted that always after correcting the intra-crustal density anomalies such as those for water, ice and sediment there are still some density anomalies left in the upper and lower mantle that we call non-isostatic (NIEs) and thermal effects. Thereby these effects should be corrected on the isostatic gravity disturbance to have a relatively pure isostatic gravity disturbance. In this section, two latter effects (i.e. NIEs and thermal effects) are investigated how much can affect gravity disturbance and subsequently Moho depth, respectively.

–Moho depths vs. sediment effects

The Earth's crust is the most heterogeneous layer which completely masks the effects of deep seated heterogeneities, especially in the observed gravity field (Tesauro et al. 2008). A problem with the isostatic Moho modelling is the uncertainty in topographic/crust density, and therefore other geophysical data are needed to constrain the density structure to overcome this problem (Tenzer et al., 2009). Ice and sediment layers (e.g., from CRUST1.0) are important data that should be considered for estimating the crustal thickness properly. For instance the effect of the sediment layers on the gravity data and crustal thickness can be observed through Figure 3. In average the sediment effects on gravity and crust estimation are 43±27.6 mGal and -2±1.3 km, respectively.

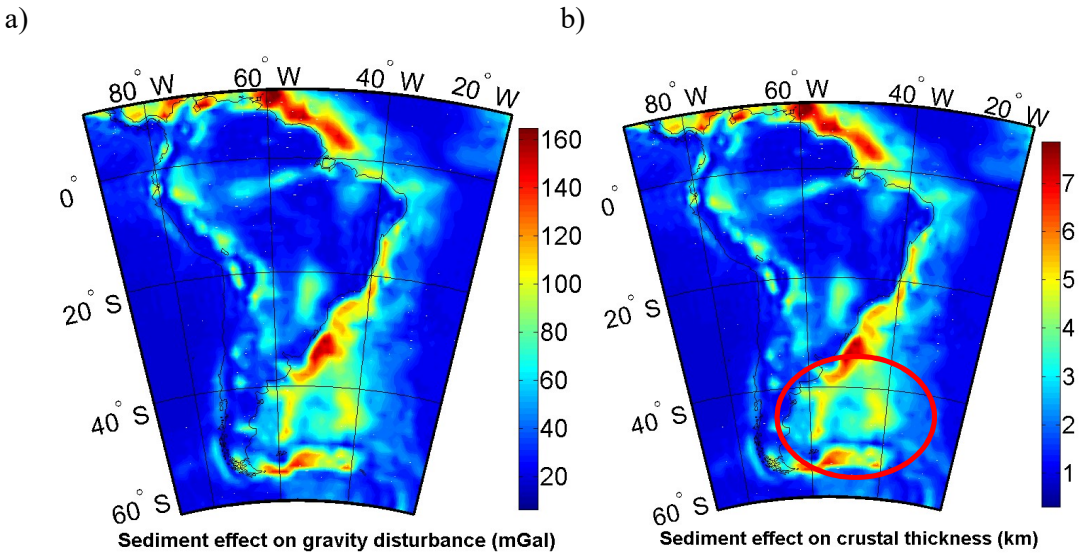

Figure 3. The effect of sediments on a) gravity disturbance (Unit: mGal) and b) crustal thickness (Unit: km) obtained from CRUST1.0 with resolution 1×1 arc-degree.

Figure 4 depicts a simple comparison with the main geological provinces of South America. The figure illustrates that the maximum sediment effects happen in Argentine Basin and East Venezuela Basin (Shelf). The minimum sediment effects located in old cratons such as Guyana, Brazilian Shields and Luis Alves cratons (2.5 to 3.8 Ga age) and belong to Archaean time. In fact they are the old and stable part of the continental lithosphere and are generally found in the interiors of tectonic plates. They are characteristically composed of ancient crystalline basement rock, which may be covered by younger sedimentary rock. Also these regions are different from that are more geologically active and unstable. The next significant of sediment effects are

observed in Famatinian Orogen and then Amazonas Basin. Generally Precambrian South American is predominantly Proterozoic in age (Cordani and Sato, 1999), and has suffered several phases of continental collision and subsequent breakup (Lioyd et al. 2010).

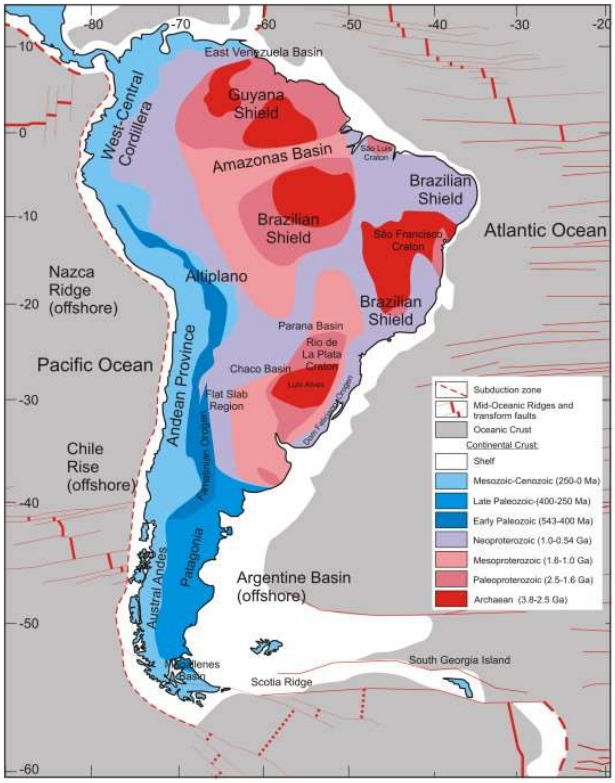

Figure 4. Main geological provinces of South America (after Chulick et al. 2013 and Gurbanov and Mooney 2012).

–*Moho depths vs. thermal effects*

As we know the outer portion of the Earth is divided into an upper, lithosphere layer, and a lower, asthenosphere layer. The lithosphere layer is composed of two parts, an upper, the crustal lithosphere and lower, the mantle lithosphere. The crustal lithosphere is in unstable mechanical equilibrium. The lithosphere layer is composed of two parts, an upper, the crustal lithosphere and lower, the mantle lithosphere. As described in Eqs. (10) and (11), the mantle density variations shallower than 125 km due to thermal expansion and pressure compression effects have been estimated, the effect on gravity disturbances has been shown in Figure 5a and the effect on crustal thickness has been shown in Figure 5b. The part deeper than 125 km has more evenly distributed density and also due to the gravity upper continuation effect, this deep part could only create very long-wavelength gravity anomalies. Therefore, we did not estimate the

density variations deeper than 125 km. The maximum values are in Mid-oceans where there is correlation between the NIE and thermal effect.

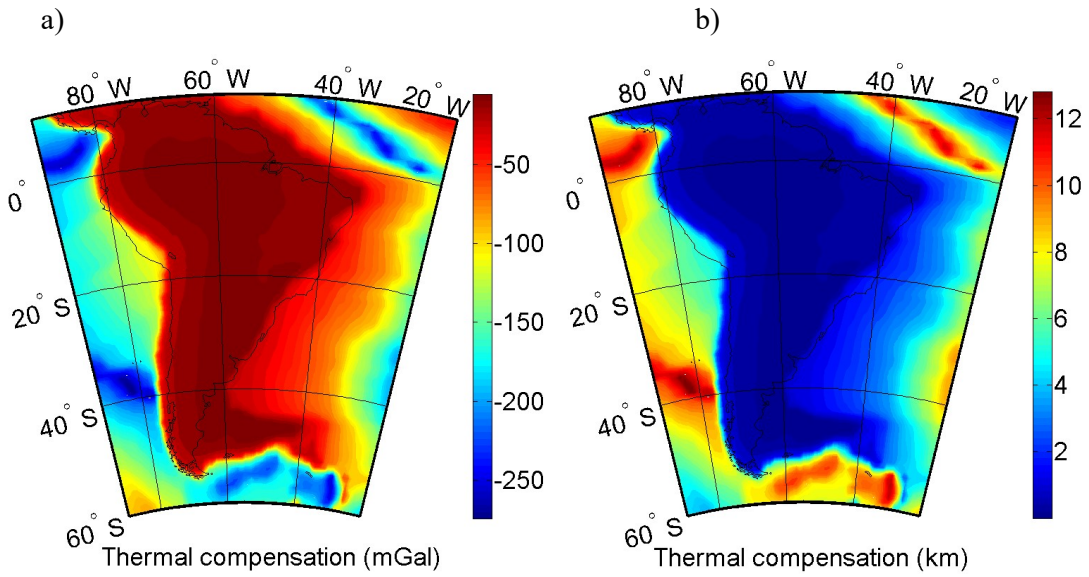

Figure 5. The effect of thermal compensation on a) the gravity disturbances, Unit: mGal and b) the crustal thickness, Unit: km, (The oceanic crustal age grid (Müller et al., 2008; Seton et al., 2012) is used for this calculation).

– *Moho depths vs. non-isostatic effects*

The contribution of the NIEs (the effect of mantle and lower masses gravity fields) on the gravity data is large as it varies between 290 to -488 with a standard deviation of 107 mGal. Understanding the NIE processes defining the mantle activity and the current state of cratons are keys for unraveling Earth's interior. The mantle and lower masses gravity field offer a starting point for numerical modeling of deeper Earth's structures and the main tool to investigate the structure of the mantle (cf. Tesauro et al. 2008). In order to investigate the reasons of significant NIE values, Fig. 4 is considered as a reference model in order to compare with the estimated NIEs in Fig. 6. The comparison shows significant NIEs values are observed in Mid-ocean ridges and transform faults in north-east and south-west of the study region (in Atlantic and Pacific Oceans). In the mid-oceans because of mantle activities the magma rising from a chamber below, forming new ocean plate which spreads away from ridge. Therefore the density of crust is higher than the other parts and this can be a good indication that the gravity field of mantle is governed in the gravity inversion for the crustal thickness determination. The next largest NIEs can be seen in Andean Province where there is a Paleozoic structure with the age of 250 and 400 Ma. Franz et al. (2006) studied evolution of the continental crust at the

central Andes. Their studies shows that growth of the continental crust is closely linked to the phenomenon of subduction (still it is ongoing process), and active continental margins (Franz et al. 2006). Therefore, the NIEs can be also used to study this phenomenon in geodynamics and behavior of entire geological systems. Generally, the positive NIE values are in oceans and the negative ones in the continental. For example, it shows that before considering the NIEs there is over-compensation (Vening Meinesz and Heiskanen, 1958) in the Andes region but the NIEs helps to reach to the isostasy assumption. The explanation and potential mechanism for over-compensation of continental crust is that the roots of over thickened crust into the mantle are larger than the topography masses.

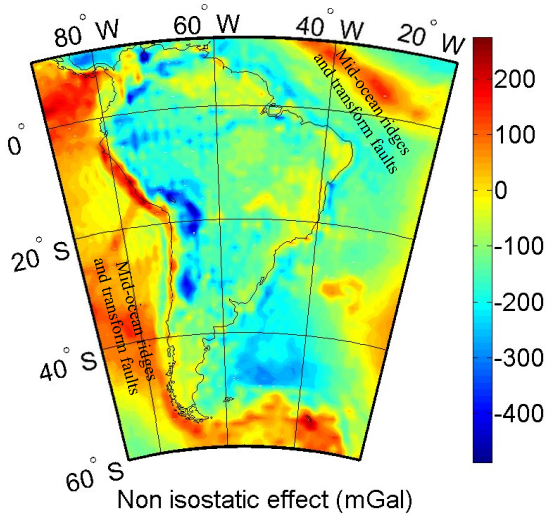

Figure 6. Non-isostatic effects after removing thermal compensation on gravity disturbance Unit: mGal.

Comparing the results presented by Kaban (2015) and the NIEs (in this study) shows that both techniques for determining mantle gravity field are consistent. The studies illustrate the impact of the masses below crust on the observed gravity field. The aim was to separate the contributions due to shallow density variations (below crust) to those related to the deep mantle from the gravity data. We know that adding the contributions of crust, lithosphere and mantle sources the resulting gravity field is correlated at more than 99% with the observed gravity (Ricard et al. 2006). Also it is important to mention that the most significant sources of the Earth's gravity field are related to the density heterogeneities associated with the topography and the Moho undulation. However one major structure of Earth's topography, the oceanic ridges, is not related to the crust but to the cooling and contraction of the oceanic lithosphere,

i.e. upper mantle (e.g. Turcotte and Schubert, 1982 and Ricard et al. 2006). Therefore the NIEs correction is very important correction in gravity inversion for Moho boundary determination. However, it is difficult to find the 3D structure of the mantle to detect the large scale density heterogeneities, but using the method presented in this study the NIEs are applicable to correct the gravity data.

–*Moho depth map corrected for NIEs and thermal effects*

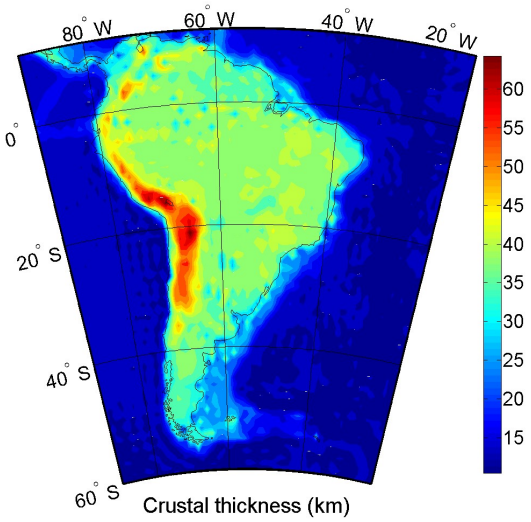

Figure 7. Gravimetric-Isostatic crustal thickness in South America with resolution of 1×1 arc-degree (corrected by the non-isostatic and thermal compensation effects). Unit: km

Figure 7 depicts the crustal thickness of South America estimated from the VMM method. The figure indicates the thicker crust along the Andes (more than 50 km) and thinner crust west of the thick craton. Average crustal thickness of the South American continent is 43.5 km which is comparable with the result presented by Chulick et al. 2013 (i.e. 45.7 km). In Figure 9 the estimated Moho depths are compared to those obtained from the CRUST1.0 model. Based on this comparison, one can see that most notable discrepancies are along the coastal zones which it could be due to the wrong initial values used and remained sediment effects in our computations for these areas. There is correlation between Figures 3 and 8 in shorelines which it shows that sediment effects were not corrected completely. One can also observe in Fig. 8 that small discrepancies are generally in mid-ocean areas which it could be attributed to the applying the NIEs and thermal effects.

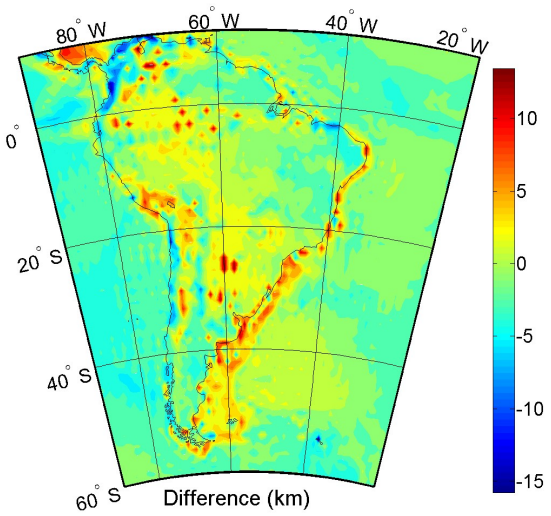

Figure 8. The difference between obtained gravimetric-isostatic and CRUST1.0 crustal thickness models with resolution of 1×1 arc-degree. Unit: km.

We used some seismic profiles for further comparison that most of them are located at the west of study region. The profiles have been reported in Assumpcao et al. (2013). Our comparison shows that the difference between the VMM model and the point-wise seismic data are less than 2 km in 70% of the points.

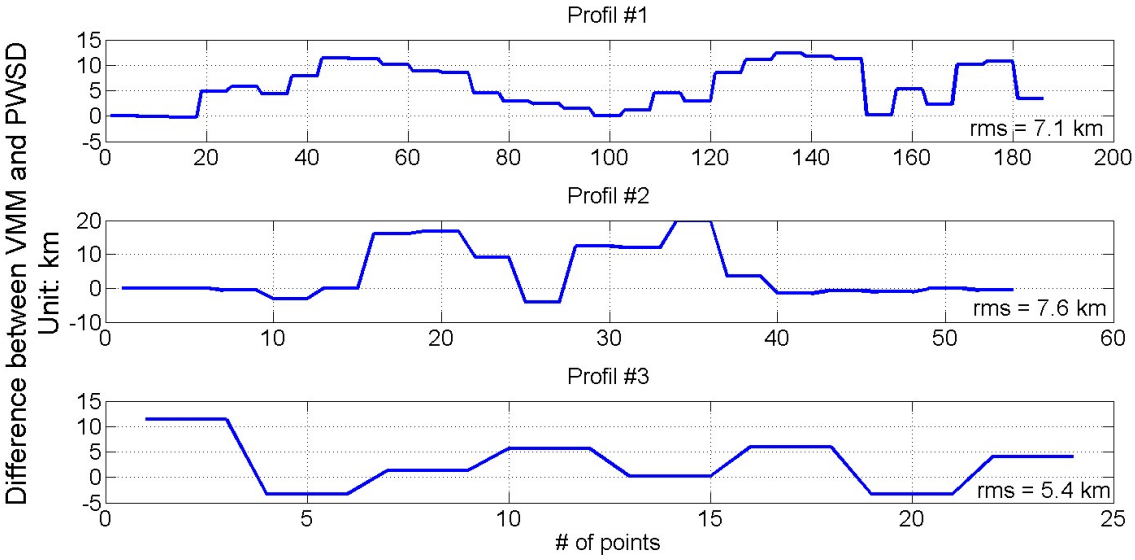

Figure 9. The difference between obtained gravimetric-isostatic and point-wise seismic data (PWSD) in three profiles presented in Figure 1.

Figure 9 illustrates the resulting three profile maps of our estimated crustal thickness compared with the point-wise seismic data in west of study region. It also shows the rms fit to the 190, 54 and 24 seismic points are 7.1, 7.6 and 5.47 km in profiles1, 2 and 3, respectively. Taking a closer look at the figure, one can observe that in profile #3 where there are good seismic data the discrepancies are relatively small, suggesting that the VMM Moho model works fairly well. However, one can also observe that the discrepancies are notable in profiles #1 and #2 with respect to profile #3, which might on one hand be due to using erroneous initial values in these areas, and on the other hand due to low quality of the seismic points in this part of the areas.

Conclusion

We have estimated crustal thickness of South America and the surrounding ocean basins using the VMM method. In addition, we firstly validated the estimated VMM Moho depths before and after applying the thermal effect and non-isostatic effects with the seismic based CRUST1.0 model. The RMS fit of the VMM Moho depths with CRUST1.0 after applying the thermal effect and non-isostatic effects was found to be 2.8 km. This RMS fit is about 40 % better than the corresponding RMS fit of 4.7 km obtained before applying the thermal effect. We then compared the VMM crustal thickness with a large number of point-wise seismic measurements. This comparison revealed that the RMS fit of the VMM Moho depths with seismic points before and after applying the thermal effect were found to be 4.5 and 4.2 km. Probable reason for this rather poor result could on one hand be attributed to using bad initial values in these areas, and on the other hand due to low quality of the seismic points in this part of the areas.

References

Afonso, J.C., Fernàndez, M., Ranalli, G., Griffin, W.L., Connolly, J.A.D., 2008. Integrated geophysical-petrological modeling of the lithosphere and sublithospheric upper mantle: Methodology and applications. Geochemistry, Geophysics, Geosystems 9, Q05008.

Assumpção, M., Bianchi, M., Julià, J., Dias, F. L., Franca, G. S., Nascimento, R., and Lopes, A. E., 2013. Crustal thickness map of Brazil: data compilation and main features. Journal of South American Earth Sciences, 43, 74-85.

Bagherbandi M., 2011. An isostatic Earth crustal thickness model and its applications. PhD thesis. Royal institute of technology. 207 pages.

Bagherbandi M. and Sjöberg L.E. ,2013. Improving Gravimetric-Isostatic Models of Crustal Depth by Correcting for Non-Isostatic Effects and Using CRUST2.0. Earth Science Review. February 2013, Pages 29Pag. Doi:10.1016/j.earscirev.2012.12.002. Doi:10.1016/j.earscirev.2012.12.002.

Bagherbandi M., Tenzer R., Sjöberg L. E., and Novak P., 2013. Improved global crustal thickness modeling based on the VMM isostatic model and non-isostatic gravity correction. Journal of Geodynamics 66 (2013) 25– 37. http://dx.doi.org/10.1016/j.jog.2013.01.002.

Bai, Y., Williams, S., Müller, R., Liu, Z., Hosseinpour, M., 2014. Mapping crustal thickness using marine gravity data: Methods and uncertainties. GEOPHYSICS 79, G27-G36.

Chapman, D.S., Pollack, H.N., 1977. Regional geotherms and lithospheric thickness. Geology 5, 265-268.

Chappell, A.R., Kusznir, N.J., 2008. Three-dimensional gravity inversion for Moho depth at rifted continental margins incorporating a lithosphere thermal gravity anomaly correction. Geophysical Journal International 174, 1-13.

Chulick G. S., Detweiler S., and Mooney W.D., 2013. Seismic structure of the crust and uppermost mantle of South America and surrounding oceanic basins. Journal of South American Earth Sciences Volume 42, March 2013, Pages 260–276.

Cordani, U., and K. Sato (1999), Crustal evolution of the South American platform, based on Nd isotopic systematics on granitoid rocks, Episodes, 22(3), 167–173.

Divins, D.L., 2003. Total Sediment Thickness of the World's Oceans & Marginal Seas, Boulder, Colo.
Dziewonski, A.M., Anderson, D.L., 1981. Preliminary reference Earth model. Physics of the Earth and Planetary Interiors 25, 297-356.

Ebbing, J., Braitenberg, C., & Götze, H. J. (2001). Forward and inverse modelling of gravity revealing insight into crustal structures of the Eastern Alps. Tectonophysics, 337(3), 191-208.

Franz Gerhard, Friedrich Lucassen, Wolfgang Kramer, Robert B. Trumbull, Rolf L. Romer, Hans-Gerhard Wilke, José G. Viramonte, Raúl Becchio, Wolfgang Siebel (2006). The Andes, Crustal Evolution at the Central Andean Continental Margin: a Geochemical Record of Crustal Growth, Recycling and Destruction. Frontiers in Earth Sciences 2006, pp 45-64

Kaban, M.K., Schwintzer, P., Reigber, Ch., 2004. A new isostatic model of the lithosphere and gravity field. J. Geod. 78, 368–385

Kaban M. (2015), Integrative gravity and isostatic models of the lithosphere and upper mantle, http://www.gfz-potsdam.de/en/section/earthsystemmodelling/topics/density-structure-of-the-earth/integrative-gravity-and-isostatic-models/. (2015-04-26).

Kimbell, G.S., Gatliff, R.W., Ritchie, J.D., Walker, A.S.D., Williamson, J.P., 2004. Regional three-dimensional gravity modelling of the NE Atlantic margin. Basin Research 16, 259-278.

Kroll, H., Kirfel, A., Heinemann, R., Barbier, B., 2012. Volume thermal expansion and related thermophysical parameters in the Mg,Fe olivine solid-solution series. Eur J Mineral 24, 935-956.

Lloyd, S., van der Lee, S., França, G.S., Assumpção, M., Feng, M., 2010. Moho map of South America from receiver functions and surface waves. J. Geophys. Res. 115, B11315. http://dx.doi.org/10.1029/2009JB006829.

Martinec, Z., 1994. The minimum depth of compensation of topographic masses. Geophys. J. Int. 117, 545–554.

Mayer-Guerr T, Rieser D, Höck E, Brockmann JM, Schuh W-D, Krasbutter I, Kusche J, Maier A, Krauss S, Hausleitner W, Baur O, Jäggi A, Meyer U, Prange L, Pail R, Fecher T, Gruber T (2012) The new combined satellite only model GOCO03s. Abstract, GGHS2012, Venice

McKenzie, D., 1978. Some remarks on the development of sedimentary basins. Earth and Planetary Science Letters 40, 25-32.

McKenzie, D., Jackson, J., Priestley, K., 2005. Thermal structure of oceanic and continental lithosphere. Earth and Planetary Science Letters 233, 337-349.

Meissner R., Mooney W., 1998. Weakness of the lower continental crust: a condition for delamination, uplift and escape. Tectonophysics 296:47–60

Moritz H., 1990. The figure of the Earth, Wichmann H., Karlsruhe.

Moritz H (1980) Advanced physical geodesy. Wichmann, Karlsruhe.

Müller, R.D., Sdrolias, M., Gaina, C., Roest, W.R., 2008. Age, spreading rates, and spreading asymmetry of the world's ocean crust. Geochemistry, Geophysics, Geosystems 9, Q04006.

Ricard, Y; Chambat, F; Lithgow-Bertelloni, C., 2006. Gravity observations and 3D structure of the Earth. CR GEOSCI , 338 (14-15) 992 - 1001. 10.1016/j.crte.2006.05.013.

Sjöberg L.E., 2009. Solving Vening Meinesz-Moritz Inverse Problem in Isostasy, Geophys. J. Int., 179, 3, 1527-1536.

Seton, M., Müller, R.D., Zahirovic, S., Gaina, C., Torsvik, T., Shephard, G., Talsma, A., Gurnis, M., Turner, M., Maus, S., Chandler, M., 2012. Global continental and ocean basin reconstructions since 200 Ma. Earth-Science Reviews 113, 212-270.

Tenzer R., Hamayun K. and Vajda P., 2009. Global maps of the CRUST2.0 crustal components stripped gravity disturbances, Journal of Geophysical Research, vol. 11, B05408, doi:10.1029/2008JB006016.

Tenzer R., Vajda P., Hamayun, 2010a. A mathematical model of the bathymetry-generated external gravitational field, Contributions to Geophysics and Geodesy, 40, 1, 31-44.

Tenzer R., Wenjin C., Tsoulis D., Bagherbandi M., Sjöberg L.E., and Novák P., 2014. Analysis of the refined CRUST1.0 crustal model and its gravity field. Surveys in Geophysics (2015) 36:139-165. DOI: 10.1007/s10712-12-014-9299-6.

Tesauro, M., M. K. Kaban, and S. A. P. L. Cloetingh (2008), EuCRUST-07: A new reference model for the European crust, Geophys. Res. Lett., 35, L05313, doi:10.1029/2007GL032244.

Turcotte, D. L., Schubert, G. (1982). Geodynamics - Application of Continuous Physics to Geological Problems. John Wiley and Sons, New York
Wang, T., J. Lin, B. Tucholke, and Y. J. Chen, 2011. Crustal thickness anomalies in the North Atlantic Ocean basin from gravity analysis, Geochem. Geophys. Geosyst., 12, Q0AE02, doi:10.1029/2010GC003402.

Watts, A.B., 2001. Isostasy and Flexure of the Lithosphere. Cambridge University Press, Cambridge, New York, Melbourne (pp. xix + 458).